Dynamic Phase Wave Propagation and Stability Characteristics in Interconnected Microgrids: A Continuum Modeling Perspective

Jiangbei Han, Member, IEEE, Xuzhu Dong, Senior Member, IEEE, Chengxi Liu, Senior Member, IEEE, Yongjian Luo, Member, IEEE, Lei Shang, Senior Member, IEEE
School of Electrical Engineering and Automation, Wuhan University, Wuhan
hanjiangbei@whu.edu.cn, dongxz@whu.edu.cn, liuchengxi@whu.edu,cn, yongjianluo@whu.edu.cn, shanglei@whu.edu.cn

***Abstract*—This paper presents a continuum modeling approach to characterize and analyze the phase wave propagation and stability characteristics in grid-type microgrid networks. By homogenizing the discrete inverter network into a quasi-continuous medium, the phase dynamics are described through coupled differential equations representing the internal grid-forming oscillators, phase-locked loops, and voltage/power control loops. A zero-reflection boundary controller (ZRC) is introduced to emulate an absorbing boundary condition that eliminates artificial reflections at the network edges, enabling the intrinsic propagation features of phase perturbations to be observed. Numerical simulations of an 8×8 interconnected microgrid demonstrate that the continuum model accurately captures the transition between grid forming (GFM)-dominant and grid following GFL-dominant behaviors, and reveals how boundary damping coefficients affect phase wave attenuation and spatial coherence. The results provide a theoretical and computational framework for phase stability assessment and spatiotemporal disturbance analysis in inverter-dominated microgrids.**

***Index Terms*—Continuum modeling, Microgrids, Grid forming (GFM), grid following (GFL).**

I. INTRODUCTION

In future power networks, the dynamic interaction among grid-forming (GFM) and grid-following (GFL) inverters within interconnected microgrids gives rise to spatial temporal phase behaviors that are fundamentally different from those in conventional synchronous power systems [1]-[2]. The phase angle of each inverter no longer represents only the mechanical rotor position as in traditional synchronous generators, but emerges as synthetic variable determined by inner current control loops, outer power/voltage control loop of inverters and network interconnections [3]. Consequently, disturbances within inverter-dominated microgrids propagate in space and time following complex coupling mechanism that resemble wave-like behaviors rather than only rotor dynamics [4].

In traditional power systems, synchronous generators are naturally synchronized through their electromechanical coupling, and phase deviations are dominated by inertia and damping of the generators. The propagation of angle disturbances is well approximated by low frequency electromechanical waves [5]-[6]. Nevertheless, in inverter-based microgrids, the physical inertia is replaced by the virtual inertia dynamics simulated by the control loop of the inverters (i.e., grid forming GFM control). This leads to a different propagation characteristic for the phase of the system. The phase synchronization speed, damping depends on control parameters rather than the mechanical properties (e.g., multi-mass block, exciting control, and speed control of the synchronous generators). In essence, analyzing the phase propagation is critical for understanding transient stability in inverter-dominated microgrid. In particular, GFM inverters behave as voltage sources defining frequency and phase autonomously, while GFL inverters rely on phase-locked loops (PLLs) to follow grid voltage [7]-[8]. The coexistence of these two types within a microgrid cluster leads to hybrid propagation phenomena: GFM nodes exhibit slower, inertia-like phase responses, whereas GFL nodes introduce faster tracking and potentially high-frequency coupling. Capturing this mixed behavior across spatially distributed microgrids requires a modeling framework that extends beyond discrete node-based systems.

The continuum modeling approach offers a promising way to describe such spatial–temporal phase dynamics. Originally developed for traditional power grids composed of synchronous machines, this method approximates the discrete network as a continuous medium governed by partial differential equations (PDEs) [9]. The grid coupling admittance and local power-angle relations are translated into continuous spatial derivatives, allowing analytical insight into disturbance propagation, attenuation, and reflection. Ref. [10] demonstrated that continuum models can effectively reveal electromechanical wave characteristics and provide closed-form relations for propagation speed and damping in large-scale synchronous systems. The main advantage of this approach lies in its ability to capture spatial coherence and global stability trends with reduced computational cost compared to full-scale discrete simulations. However, its application to inverter-based microgrids has been limited, as the intrinsic fast dynamics, PLL synchronization, and control-mode diversity break the uniformity assumptions used in classical formulations.

Unlike synchronous systems, microgrids exhibit heterogeneous inverter dynamics, non-uniform damping, and mixed GFM/GFL operation, resulting in locally varying phase wave speeds and boundary conditions. Furthermore, microgrids are

This work was supported by the 2030 National Science and Technology Major Project (2025ZD0804802), the National Natural Science Foundation of China under Project U22B20100. (*Corresponding author*: *Xuzhu Dong*)

J. Han, X. Dong, C. Liu, J. Luo and L. Shang are with the School of Electrical Engineering and Automation, Wuhan University, Wuhan, Hubei 430072, China

often operated in meshed topology configurations with finite boundaries, where reflected phase waves can distort synchronization and stability assessments. Traditional continuum models cannot directly account for these hybrid dynamics or reflective boundaries. To address these challenges, it is necessary to extend the continuum framework by incorporating control-dependent parameters such as the PLL gain, virtual damping. Such an enhanced formulation enables analysis of phase wave propagation, reflection, and absorption in inverter-dominated systems. This paper focuses on developing and analyzing a continuum-based phase propagation model for interconnected microgrids with mixed GFM and GFL dynamics. The main contributions are as follows:

1) Based on the continuum modeling approach, a hybrid phase dynamic model of the inverters-dominated microgrids is established that considers the dynamic behaviors of GFM and GFL through control-dependent parameters.
2) A time-ramped zero-reflection boundary controller is designed for the inverters of the battery energy storage system (BESS) to emulate absorbing boundaries, enabling the observation of natural phase propagation within a finite microgrid domain.
3) Simulation results on an 8×8 interconnected microgrid demonstrate how the continuum-inspired model captures the transition between GFM-dominant and GFL-dominant regions and provides insights into phase stability and wave attenuation mechanisms.

It is noted that the proposed continuum model is intended as a theoretical and analytical framework for investigating spatial–temporal phase propagation and stability mechanisms in inverter-dominated systems. Despite simplifying assumptions on network density and phase gradients, the model provides valuable physical insight into disturbance propagation, boundary reflection, and damping mechanisms, which are of direct relevance to power system dynamic stability analysis.

II. Hybrid Phase Dynamic Model of the Inverters Dominated Microgrids

This section extends the classical electromechanical continuum theory to inverter-dominated microgrids, bridging synchronous-generator physics and converter control dynamics. The resulting hybrid phase dynamic model captures the essence of spatial–temporal interactions in complex microgrid networks,

A. The Continuum Model of Traditional Power Systems

In conventional synchronous power systems, the electromechanical dynamics of generators can be described by the well-known swing equation. For the i-th machine, the dynamic equations are expressed as

$$\begin{cases} M_i \dot{\omega}_i = P_{m,i} - P_{e,i} - D_i(\omega_i - \omega_s) \\ \dot{\delta}_i = \omega_i - \omega_s \end{cases} , \tag{1}$$

where M_i and D_i are the inertia and damping constants, respectively, $P_{m,i}$ is the mechanical input power, $P_{e,i}$ the electrical output power, and ω_s is the synchronous reference frequency. When considering a large interconnected grid, the coupling power term $P_{e,i}$ can be approximated as

$$P_{e,i} = \sum_j K_{ij} \sin(\delta_i - \delta_j) , \tag{2}$$

where $K_{ij}=|V_i||V_j|B_{ij}$ represents the synchronizing strength between buses i and j. If the system is densely meshed and the angle difference between neighboring nodes is small, the network can be represented by a continuous field $\delta(x,y,t)$. Using spatial discretization and Taylor expansion, the swing equations lead to a continuum approximation:

$$M \frac{\partial^2 \delta}{\partial t^2} + D \frac{\partial \delta}{\partial t} = K \nabla^2 \delta \tag{3}$$

Eq. (3) is the damped wave equation governing phase propagation. The term $K\nabla^2\delta$ corresponds to the phase stiffness of the grid, while M and D determine wave inertia and damping. This model explains how power-angle disturbances propagate as electromechanical waves with finite velocity, which is a phenomenon extensively observed in large-scale transmission networks.

B. The Continuum Model of GFL and GFM Inverters

In inverter-based microgrid as shown in Fig. 1, each inverter in the point of common coupling (PCC) bus of this microgrid is integrated with a distributed generator (DG) unit such as wind turbine, PV or the battery energy storage system (BESS). The physical inertia of synchronous generator is replaced by the synthetic dynamics of inverter control loops. Two dominant control modes determine the local phase behavior, which are grid-following (GFL) and grid forming (GFM) inverters.

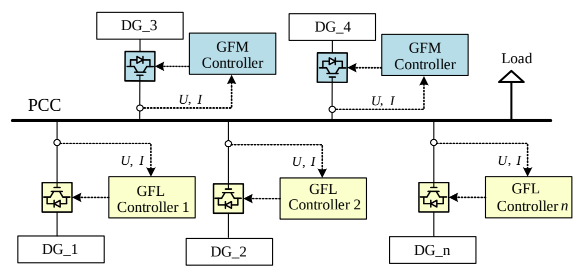

Fig. 1.The typical topology of the inverter-dominated microgrid.

The control strategy of the GFM inverter emulates the dynamics of voltage source, which can be expressed as

$$\begin{cases} M_v \dot{\omega} = P_{set} - P - D_v \omega \\ \dot{\delta}_{gfm} = \omega \end{cases} , \tag{4}$$

where M_v and D_v represent virtual inertia and damping. The GFM unit maintains a stable voltage magnitude and acts as a source of reference phase, supporting grid synchronization. The GFL inverters operate as controlled current sources based on the phase-locked loop (PLL), whose dynamics can be expressed as

$$\dot{\delta}_{pll} = \alpha_{pll}(\theta_{pcc} - \delta_{pll}) , \tag{5}$$

where α_{pll} is the PLL bandwidth and θ_{pcc} is the measured terminal angle. Large α_{pll} values lead to fast tracking (GFL-type), while small α_{pll} values imply slow following behavior, approximating GFM-type response. For a network of converters, the electrical coupling can be similarly expressed as

$$P_i = \sum_j K_{ij} V_i V_j \sin(\delta_i - \delta_j) , \tag{6}$$

979-8-3315-8138-1

By applying the continuum approximation again and introducing the node-dependent hybrid phase $\delta(x,y,t)$, the GFM and GFL dynamics can be combined into following equation

$$\begin{aligned} & M(x,y)\frac{\partial^2\delta}{\partial t^2}+D(x,y,t)\frac{\partial\delta}{\partial t} \\ & =K(x,y)\nabla^2\delta-\alpha_{pll}(x,y)[\delta(x,y,t)-\theta(x,y,t)] \end{aligned}, \quad (7)$$

where $D(x,y,t)$ includes time-ramped absorbing boundaries and $\alpha_{pll}(x,y)$ represents spatially varying PLL stiffness across the microgrid. Eq. (7) bridges inverter control and spatial phase propagation, revealing that converter dynamics directly modulate the local phase wave properties (including wave speed, attenuation, and reflection).

C. The Hybrid Phase Dynamic Model of Inverters Dominated Microgrids

The last part introduces the typical inverter-dominated microgrid, in practical system, such a microgrid can be defined as a node of microgrids and both GFM and GFL inverters coexist, forming heterogeneous spatial fields in different node. A hybrid microgrids is shown in Fig. 2.

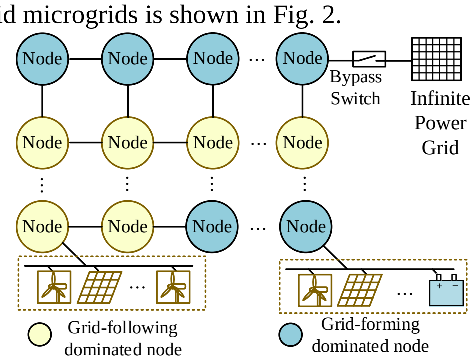

Fig. 2. A hybrid inverter-dominated microgrids with multiple GFL and GFM nodes.

Each node in Fig. 2 can be represented as a hybrid system with the effective phase, which is

$$\delta_{hyb}=(1-\alpha_i)\delta_{gfm,i}+\alpha_i\delta_{pll,i}\,. \quad (8)$$

In (8), α_i indicates the inverter's dominance type. The value of α_i is in the range of 0 to 1. Substituting (8) into the network equations yields the following hybrid phase dynamic model.

$$\begin{cases} \dot{\delta}_{gfm,i}=\omega_i \\ \dot{\omega}_i=P_{set,i}-P_i-D_i(t)\omega_i \\ \dot{\delta}_{pll,i}=\alpha_i(\theta_i-\delta_{pll,i}) \\ \dot{V}_i=k_{v,i}(Q_{set,i}-Q_i) \end{cases} \quad (9)$$

By stacking these equations for all nodes and coupling via the admittance matrix Y, the microgrid becomes a spatially distributed nonlinear system whose collective phase behavior exhibits: 1) Localized excitation and wave propagation, analogous to electromechanical waves but governed by virtual inertia and control delays; 2) Boundary reflection and absorption, controlled by damping $D_i(t)$; 3) Mode hybridization, as GFM nodes act as sources and GFL nodes as absorbers of phase energy. In the continuum limit, the hybrid phase evolution obeys

$$\begin{aligned} & M_{eq}(x,y)\frac{\partial^2\delta_{hyb}}{\partial t^2}+D_{eq}(x,y,t)\frac{\partial\delta_{hyb}}{\partial t} \\ & =K_{eq}(x,y)\nabla^2\delta_{hyb}+S_{ctrl}(x,y,t) \end{aligned}, \quad (10)$$

where S_{ctrl} is the inverter control coupling terms (PLL and P/Q loops). The hybrid phase continuum model enables analytical treatment of microgrid-wide phase wave propagation, and provides physical insight into how local converter control parameters (e.g., damping, PLL bandwidth, power droop gains) affect the global synchronization and spatial stability.

III. Time-Ramped Zero-Reflection Boundary Controller

In both conventional power networks and inverter-dominated microgrids, reflections of phase waves at network boundaries or impedance mismatches can lead to undesirable oscillations and power sharing instability. When a phase disturbance (e.g., a transient power imbalance) travels toward the edge of the network, part of the wave energy may reflect back into the interior region, interfering with ongoing oscillations. To suppress such reflection phenomena, a zero-reflection boundary controller (ZRC) is introduced in this section. This controller is inspired by absorbing boundary conditions used in continuum mechanics and electromagnetic wave propagation, and is adapted here for phase wave absorption in inverter-dominated microgrids.

The damping coefficient in (10) is spatially and temporally modulated as

$$D(x,y,t)=D_{base}+[D_{max}(x,y)-D_{base}].f(t)\,, \quad (11)$$

where D_{base} is the nominal damping for internal nodes. $D_{max}(x,y)$ is the maximal edge damping coefficient, spatially distributed according to the distance from the network boundary.

$$D_{max}(x,y)=D_{base}+[D_{edge}-D_{base}].\left[1-\frac{d(x,y)}{L}\right]^+, \quad (12)$$

where $d(x,y)$ denotes the number of nodes between a given node and the nearest network edge, and L is the absorbing layer thickness (typically 1 to 2 nodes in discrete simulation).The operator $[.]^+$ensures that the value saturates at zero for interior nodes beyond the damping layer. Thus, edge nodes experience stronger damping, while inner nodes retain the original low damping. The result is a spatially graded "absorbing layer" that eliminates boundary reflections similarly to a perfectly matched layer in electromagnetic simulations. $f(t)$ is the time-ramping function controlling the smooth activation of the absorber, which can be expressed as

$$f(t)=\begin{cases} t/T_r, & 0\le t\le T_r \\ 1, & t\ge T_r \end{cases}, \quad (13)$$

where T_r is the ramp-up time constant, which ensures a continuous and reflection-free transition from an initially undamped boundary to the fully absorbing state.

Physically, the ZRC is implemented through adaptive damping injection at the microgrid periphery using existing inverter control loops, rather than introducing an independent controller. In practice, this damping can be realized by adjusting virtual damping or virtual impedance terms in grid-forming inverters, fast power–frequency damping in boundary battery energy storage converters, or effective damping enhancement in grid-following inverters through

979-8-3315-8138-1

PLL-related control parameters. The ZRC relies only on local measurements of frequency or phase angle, which are already available in standard inverter control structures, and does not require additional communication. By continuously ramping the damping term $D(x,y,t)$ from zero to its maximum at the boundaries, outgoing phase waves are gradually absorbed.

IV. Case Study and Results Analysis

A. Conventional Synchronous Generator Network

To validate the phase propagation mechanism under the synchronous generator-dominant power system, a benchmark network composed of interconnected synchronous generators is considered. The system consists of a 35×35 nodal lattice, where each node represents an equivalent generator with swing dynamics governed by the classical second-order model (given in Eq. (1)), The initial equilibrium satisfies the steady-state power flow condition, and at t=0, a localized active power disturbance is applied to the center node, initiating a spatial phase disturbance that propagates outward across the network.

The first scenario (shown in Fig. 3) depicts the uncontrolled case, where the network boundary is reflective [10]. At the initial instant (t=0), a single-phase spike appears in the center of the domain, corresponding to the directly excited node. As time evolves (t=0.5–20s), the disturbance propagates radially outward as coupled oscillatory waves. Due to the reflective boundary, these waves are partially reflected at the system edges and interfere with incoming waves, forming a complex standing-wave pattern. At later stages (t>15s), the system exhibits multiple interference fringes and slow decay, which are characteristic of the high inertia and low damping nature of synchronous generator networks. The power-angle oscillations retain their global coherence but demonstrate long-lasting spatiotemporal coupling.

In the second scenario (shown in Fig. 4), a ZRC is applied to the boundary nodes, which is achieved by adjusting the damping coefficient of the synchronous generators at the edge nodes in practical system. The damping coefficient near the edges is increased gradually according to (14).

$$D_{sync}(x,y,t) = D_0 + D_{mac\_sync}\left(\frac{t}{T_{ramp}}\right)\Gamma(x,y) \tag{14}$$

In (14), $\Gamma(x,y)$ is a spatial weighting function that peaks near the outermost nodes. This configuration aims to absorb outgoing phase waves, preventing reflection and preserving the physical behavior of an infinite system. The results of phase evolution demonstrate a clear improvement. The initially excited phase perturbation propagates outward, but the reflected waves are largely suppressed. The phase field gradually returns to a smooth equilibrium, and the residual oscillation energy is dissipated monotonically through the ZRC layer. Compared with the uncontrolled case, the zero-reflection boundary yields a unidirectional phase attenuation profile, reproducing the theoretical prediction of continuum-wave absorption in finite domains.

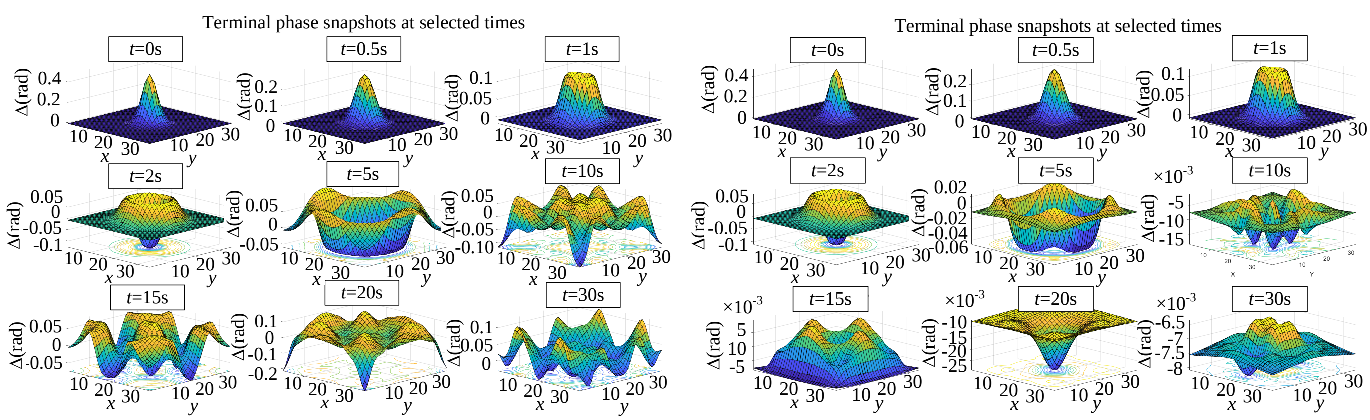

(a) Synchronous Generator Network Without ZRC (b) Synchronous Generator Network With ZRC

Fig. 3. Time snapshots of phase propagation as a function of position in a 35×35 grid system without or with zero-reflection controllers placed on the edges of the network.

B. Hybrid Inverter-Dominated Microgrids

An inverter-dominated microgrid network is modeled to investigate the spatial–temporal phase behavior of inverter-based systems. The network adopts the 8×8 lattice topology to facilitate direct comparison, but each node now represents an equivalent microgrid port that integrates both GFM and GFL inverter dynamics. The grid topology is 8×8 lattice including 64 nodes, the inner 32 nodes are GFM-dominant (α_i in Eq. (8) is set as 0.2), while the outer 32 nodes are GFL-dominant (α_i in Eq. (8) is set as 0.8). Then, a small power pulse applied to the central node at t=0. The first case (shown in Fig. 4(a)) shows the microgrid phase propagation without zero-reflection control. Initially, a smooth spatial gradient form around the excitation point, unlike the sharp peak in the synchronous system (shown in Fig. 3(a)). This is due to the inverter control bandwidth, where PLL and voltage loops inherently diffuse fast transients. Then, a disturbance was observed to propagate outward as a phase wave through the inverter-based network. Upon reaching the boundary of the isolated microgrid, the wavefront reflected back into the system, leading to the formation of distinct interference patterns that persisted for multiple seconds. The second case (shown in Fig. 4(b)) introduces the time-ramped zero-reflection controller at the outermost boundary by adding the damping control loop in the control of

979-8-3315-8138-1

the inverters at the edge nodes in practical system. As predicted by the continuum theory, the ZRC effectively absorbs outgoing phase waves, allowing energy to dissipate smoothly. The phase snapshots illustrate a monotonic attenuation of the disturbance: when t=0, a localized phase bulge appears at the disturbance center. When t=5s, the wavefront expands with minimal back-reflection. After t=20 s, the phase field becomes nearly flat, indicating full damping of the perturbation. Although only absolute phase values are shown, the absence of spatial phase ripples and reflected wavefronts implies the decay of phase gradients, which is dynamically consistent with suppressed frequency deviations under the proposed ZRC.

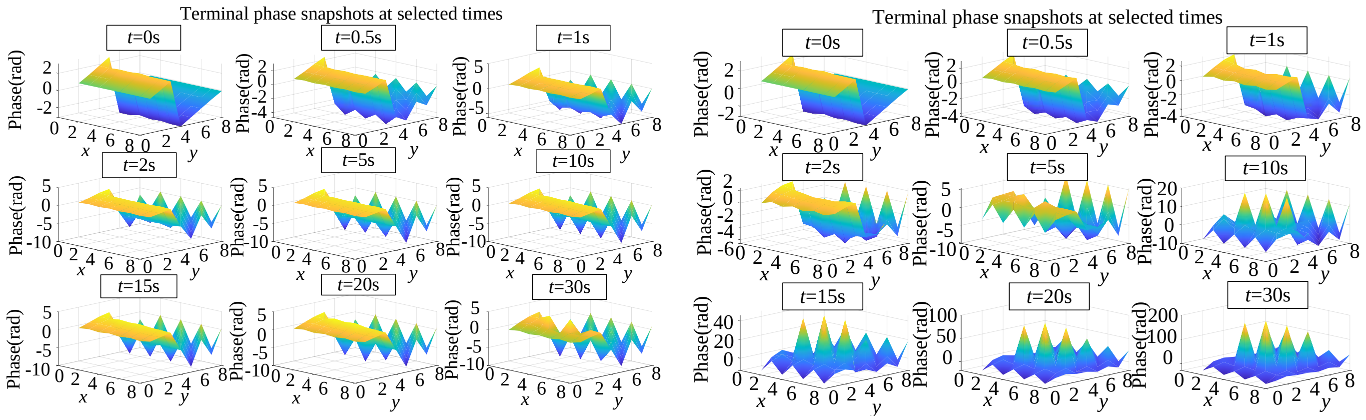

(a) Hybrid Inverter-Dominated Microgrids Without ZRC (b) Hybrid Inverter-Dominated Microgrids With ZRC

Fig. 4. Time snapshots of phase propagation as a function of position in a 8×8 grid system without or with zero-reflection controllers placed on the edges of the network.

V. Advantages and Limitations of the Continuum Modeling Approach in Microgrids

A. Advantages

The continuum modeling approach provides a unified and intuitive framework for describing spatial–temporal phase behaviors in inverter-dominated microgrids. Compared with conventional discrete node-based models, it offers following benefits:

1) By treating spatially distributed converter nodes as a continuous phase field, the model transforms complex algebraic coupling into a partial differential equation (PDE) form, revealing collective propagation and synchronization behaviors.
2) The phase field captures how disturbances spread, reflect, and dissipate through the network—phenomena difficult to see in standard small-signal or eigenvalue analyses. This enables systematic design of spatial damping strategies such as the time-ramped ZRC.
3) The same continuum formulation links synchronous generator electromechanical waves and converter-induced phase dynamics, supporting analytical comparison and transfer of control concepts between the two domains.

B. Limitations

Despite its clarity, the continuum method has several practical constraints:

1) Real microgrids are heterogeneous and sparse, the continuous assumption may miss localized effects or nonuniform line parameters.
2) The PDE form assumes small phase gradients and weak coupling, which may fail under large disturbances.
3) Real-time measurement of continuous phase fields remains challenging, hindering experimental confirmation.

VI. Conclusions

This paper has developed a hybrid phase dynamic framework for understanding the spatial-temporal behavior of inverter-dominated microgrids. By extending the continuum modeling approach to microgrid systems comprising grid-forming (GFM) and grid-following (GFL) converters, we have revealed how phase propagation in microgrids fundamentally differs from that in conventional power systems.

In future work, we will establish more detailed equivalent models to investigate the impact of different grid-forming (GFM) and grid-following (GFL) ratios, control parameters, and operating conditions on phase propagation in microgrids. Additionally, we will design adaptive zero-reflection controllers to effectively suppress phase transfer and maintain microgrid stability.

References

[1] G. Hu et al., “An extended impedance model for power electronics converters retaining explicit synchronization dynamics,” *IEEE Trans. Power Electron.*, vol. 40, no. 1, pp. 2355-2370, Jan. 2025.

[2] Y. Li, Y. Gu, T. Green, Revisiting grid-forming and grid-following inverters: a duality theory,” *IEEE Trans. Power Syst.*, vol. 37, no. 6, pp. 4541-4554, Nov. 2022.

[3] H. Ding, R. Kar, Z. Miao, L. Fan, A novel design for switchable grid-following and grid-forming control, *IEEE Trans. Sustain. Energy*, vol. 16, no. 2, pp. 1301-1314, April 2025.

[4] H. Cui *et al.*, "Disturbance Propagation in power grids with high converter penetration," *Proc. of the IEEE*, vol. 111, no. 7, pp. 873-890, July 2023.

[5] Y. Xu, F. Wen, G. Ledwich and Y. Xue, “Electromechanical wave in power systems: theory and applications,” *Journal of Modern Power Systems and Clean Energy*, vol. 2, no. 2, pp. 163-172, June 2014.

[6] A. Esmaeilian, M. Kezunovic, Impact of electromechanical wave oscillations propagation on protection schemes, *Electric Power Systems Research*, vol. 138, pp. 85-91, 2016.

[7] D. Espín-Sarzosa et al., “Microgrid modeling for stability analysis,” *IEEE Trans. Smart Grid*, vol. 15, no. 3, pp. 2459-2479, May 2024.

[8] Wang, J., et al., “Study of inverter control strategies on the stability of microgrids,” NREL Technical Report, 2023.

[9] D. Wang, X. Wang and J. Thorp, “Study on electromechanical wave continuum model for power systems in mechanics,” 2006 *IEEE Power Engineering Society General Meeting*, Montreal, QC, Canada, 2006, doi: 10.1109/PES.2006.1709216.

[10] Huang, L., “Electromechanical wave propagation in large electric power systems,” Virginia Tech, 2003.

979-8-3315-8138-1